Prospects of the Intrajet radiation studies in ALICE experiment

O. Driga
Subatech, Nantes
21.09.2010

Outline

- Theoretical background
- Outlook of previous experiments
- Perspectives for ALICE
- Numerical estimations
- Plans for the future

QED: the essence of coherence

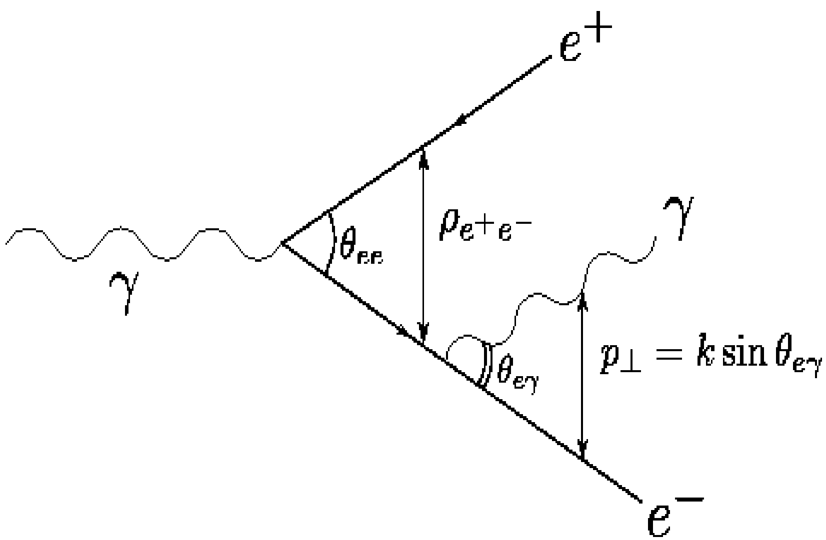

- To which extent e+ and e- independently emit gamma's?

- If the wavelength of the photon is larger than the transverse separation of e+e-, it cannot resolve the internal structure of the pair and probes only the electric charge, i.e. is effectively emitted by the chargeless object -> emission suppressed

$$\lambda_{\perp\gamma} = \frac{1}{p_\perp} = \frac{1}{k\Theta_{e\gamma}} \;; \qquad \rho_{e^+e^-} = \lambda_{\perp\gamma}\frac{\Theta_{ee}}{\Theta_{e\gamma}}$$

$$\rho_{e^+e^-} \ll \lambda_{\perp\gamma}, \quad \text{when} \quad \frac{\Theta_{ee}}{\Theta_{e\gamma}} \ll 1$$

The emission at large angles is suppressed (Chudakov effect)

A.E. Chudakov. ***Izv. Akad. Nauk SSSR*, Ser. Fiz., 19:650, 1955.**

QCD: color coherence

•The same effect takes place in QCD where soft gluon radiation is governed by conserved color currents.

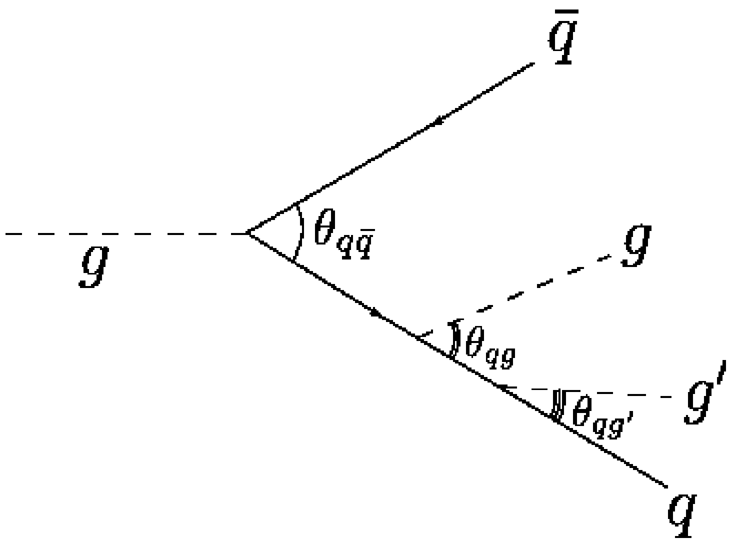

•On the one hand, the wavelength of the emitted gluon should be smaller than the hadronization scale R:

$$\lambda_{\perp g} = \frac{1}{k \sin \Theta_{qg}} > R \Rightarrow \Theta_{qg} > \frac{1}{kR}$$

•On the other hand, we have angular ordering:

$$\Theta_{qq} \ll \Theta_{qg} \ll \Theta_{qg'}$$

Yu.L. Dokshitzer, V.A. Khoze, A.H. Mueller, and S.I. Troyan. *Rev. Mod. Phys.*, 60:373, 1988.

What can we observe with color coherence?

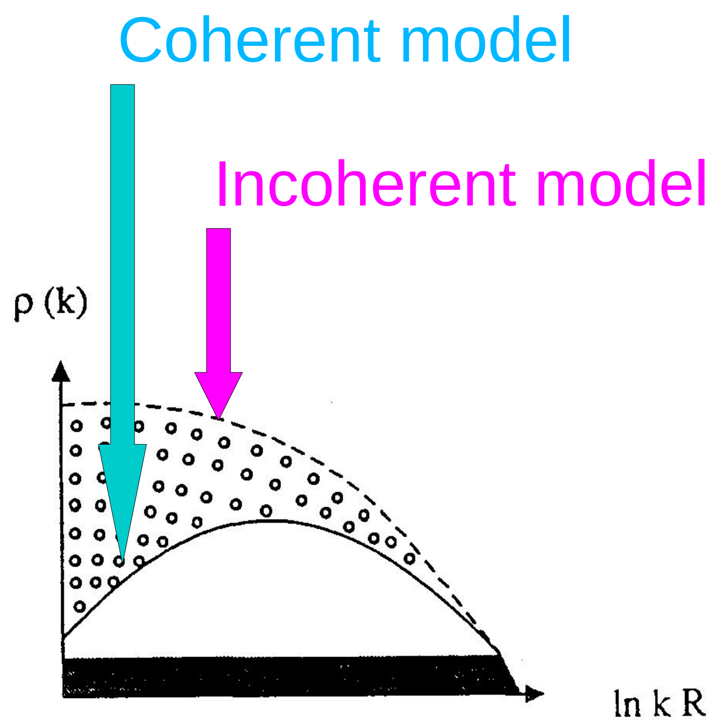

Particle energy spectrum

$$\rho(k) \equiv \frac{dn}{d\ln k}$$

R – hadronization scale,
k – particle momentum

- Let us illustrate the influence of color coherence on particle spectra on a toy model
- The suppression of soft radiation follows from the angular ordering of partonic cascade and is a direct manifestation of the color coherence.
- This can be understood on kinematics ground as a result of two conflicting tendencies: due to the hadronization a slow particle is 'forced out' at large emission angle, on the contrary, the allowed decaying angle, after a few successive branching, is shrunk to small values.

Ya.I. Azimov, Yu.L. Dokshitzer, V.A. Khoze, and S.I. Troyan. *Z. Phys.*, C31:213, 1986.

Energy spectrum of Particles in jets: MLLA and LPHD hypothesis

- The Modified Leading Log Approximation formalism (MLLA)
- Why LLA?

Considers only leading contribution to the multiparton cross sections.

$$\sigma : \quad \frac{\alpha_s}{\pi} \log^2 Q^2 \sim 1, \quad \frac{\alpha_s}{\pi} \log Q^2 \ll 1, \quad \frac{\alpha_s}{\pi} \ll 1$$

Double Log – Leading Contribution   Single log – Non-leading

- Why Modified?

Supposition that all the essential interference terms between Single and Double logarithmic terms can be neglected

- How are we going to observe gluon distributions?

Supposition of the Local Parton-Hardron Duality (LPHD):
Similar behaviour of the hadronic spectra and parton distributions

Ya.I. Azimov, Yu.L. Dokshitzer, V.A. Khoze, and S.I. Troyan. ***Z. Phys.***, **C27:65, 1985.**

CDF: fragmentation function vs M_{jj}

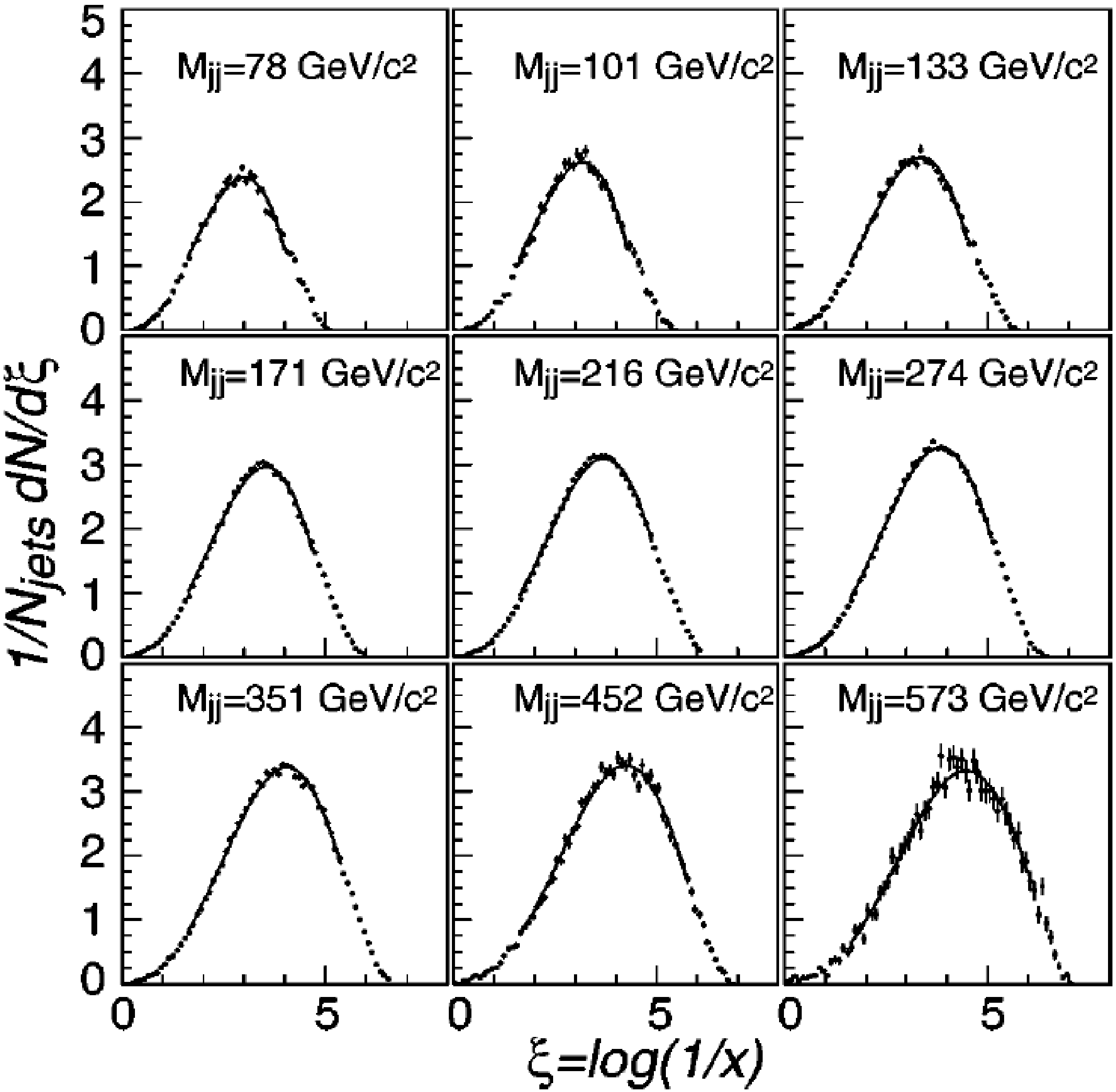

- Inclusive momentum distribution of particles in jets in the restricted cone of size θ_c=0.47.
- The line represents the fit of the data to the MLLA gluon spectrum.
- $x=p_t^{part}/p_t^{jet}$

CDF collaboration. Phys.Rev.D68, 012003 (2003)

What can be learned from the previous experiments

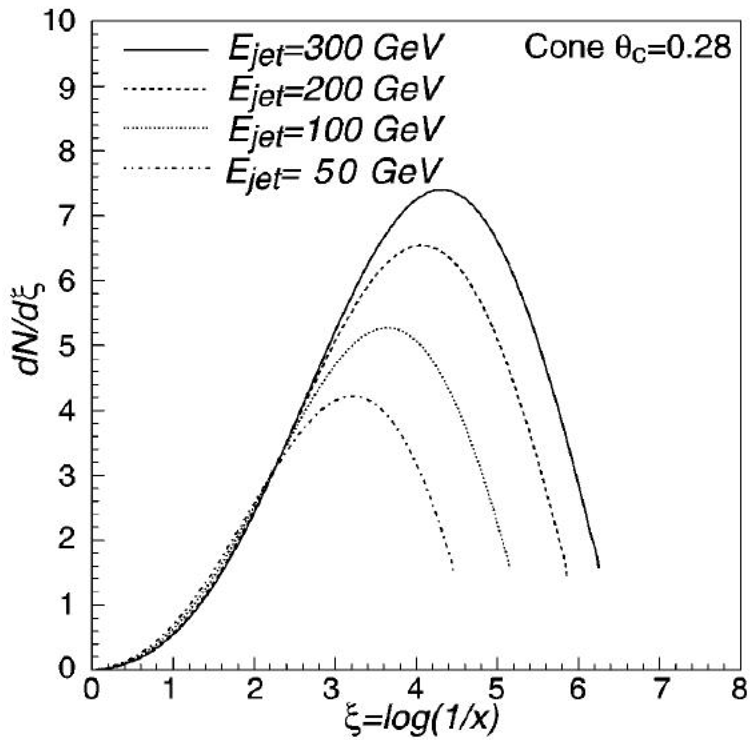

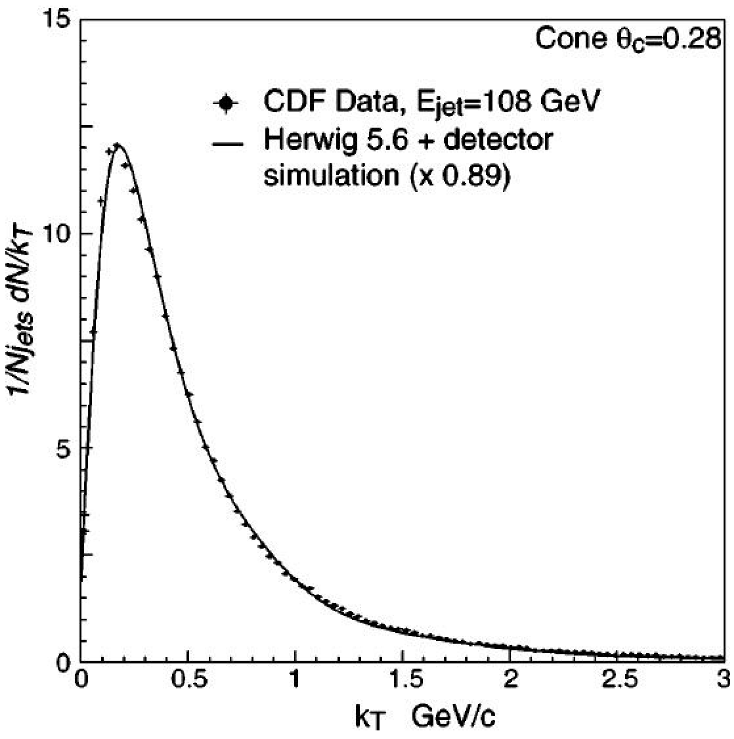

- Several observable were measured: D(x), D(ξ), ξ_0, k_T, particle multiplicity in jets.
- MLLA introduces the new phenomenological scale Q_{eff} replacing Λ_{QCD} and Q_{cutoff}. Q_{eff} can be deduced from ξ_0 value.
- Jet measurements in e^+e^- colliders, e^-p, $p\bar{p}$ colliders are consistent and correspond well with MLLA
- Particle distribution in jets confirm color coherence.

ALICE: Event Topology

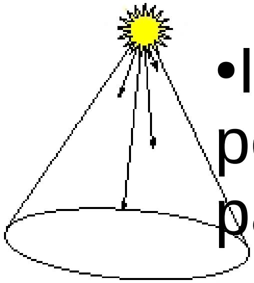

- Ideally, to study particle distribution in a jet, one has to perform an accurate measurement of the energy of each particle and the total jet energy (“inclusive jet events”).

- In practice, jet energy measurement is strongly affected by finite jet finding capability of the detector.

Dijets detection might improve jet energy measurement.

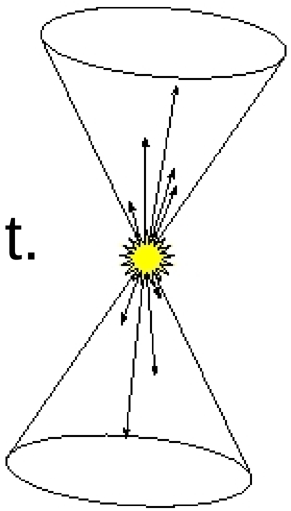

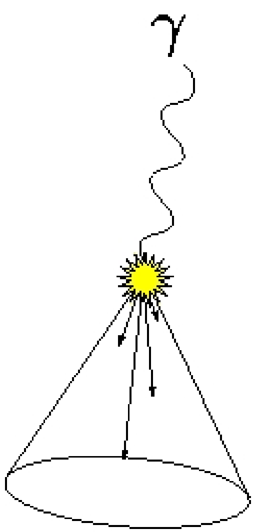

- Photon tagging of a jet can improve jet energy measurement even more.

Statistics

Energy resolution

ALICE and Intrajet radiation

ALICE can go to large ξ values

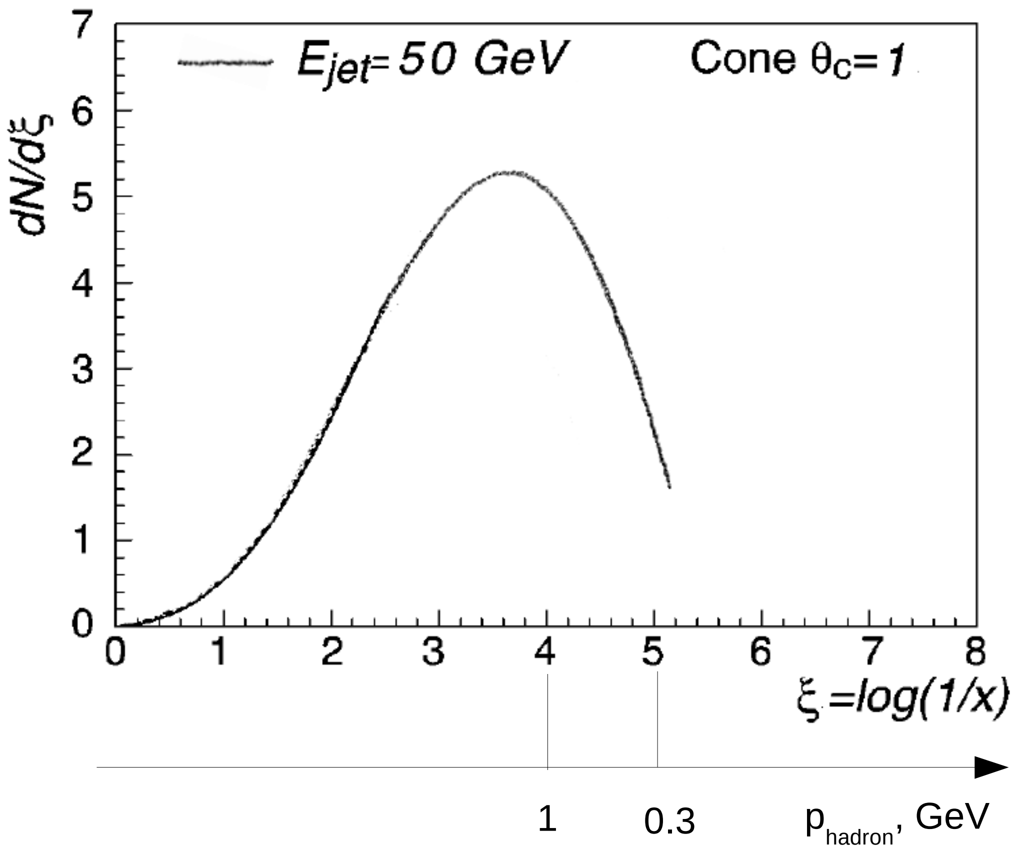

•$x=E^{part}/E^{jet}$, $dN/d\xi$ ~ particle density
•Measurement of the small p_t region can be promising for ALICE

•For feasibility study of the intrajet radiation we need to measure several observables: the energy of the jet E_{jet}, the energy of each particle E_p, and the particles density.
•On the other hand, we have to keep in mind the main obstacles: error bars:

•Particle reconstruction efficiency and finite particle momentum resolution
•Jet energy measurement uncertainties (driven by acceptance effect, background, out-of-cone fluctuations, etc)
•Statistical uncertainty

Particle reconstruction efficiency

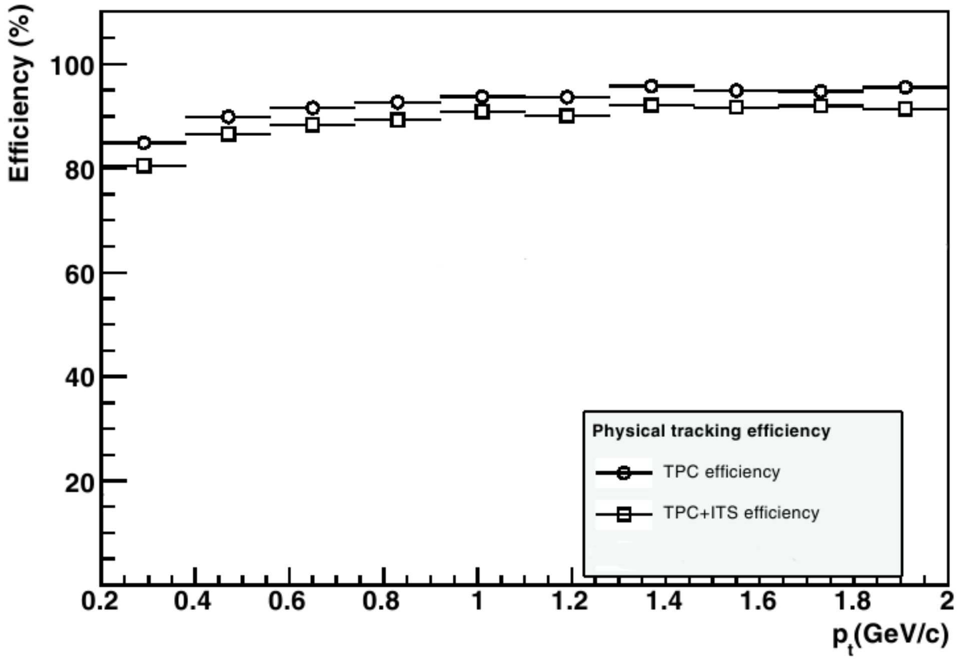

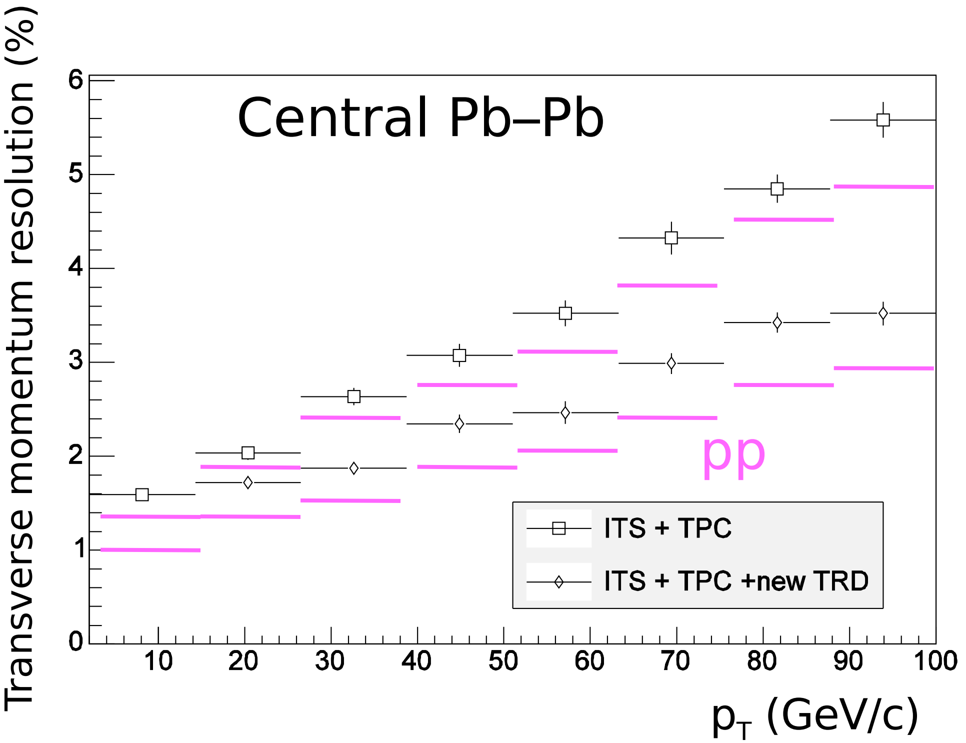

Charged particles

- Central barrel: |η| < 0.9, delta phi = 2 pi
- Optimized for high multiplicity (8000 particles)
- Tracking down to 100 MeV/c.
- Excellent track reconstruction up to 100 GeV/c
- p_T resolution better than 10% until 100 GeV/c

Neutral particles

- PHOS : dE/E = 0.025/E + 0.030/√E + 0.011
- EMCAL: dE/E = 0.051/E + 0.11/√E+ 0.017

Parameters of simulation

- Event generator: Pythia v.6.214 within aliroot
- Collision system: proton-proton $\sqrt{s}$=7 TeV
- $p_{t\text{-}hard}$ limits: from 10 to 130 with 10-GeV bins (12 bins)
- Subprocesses:
  - gamma-jet events: direct photons (MSEL=10)
  - inclusive jet events: hard QCD processes (MSEL=1)
  - dijet events: hard QCD processes (MSEL=1)

- Generated statistics: $12*10^6$ events for monojet, dijet and gamma-jet

- Jet finding: Pycell
  - R_{jet} = 0.4
  - $|\eta|<0.9-R_{jet}$
  - cell size (à la EMCAL): $\Delta\varphi=0.014$, $\Delta\eta=0.014$
  - E_{seed}: 4 GeV
  - E_{cutoff}: 2 GeV

Inclusive jet counting rates

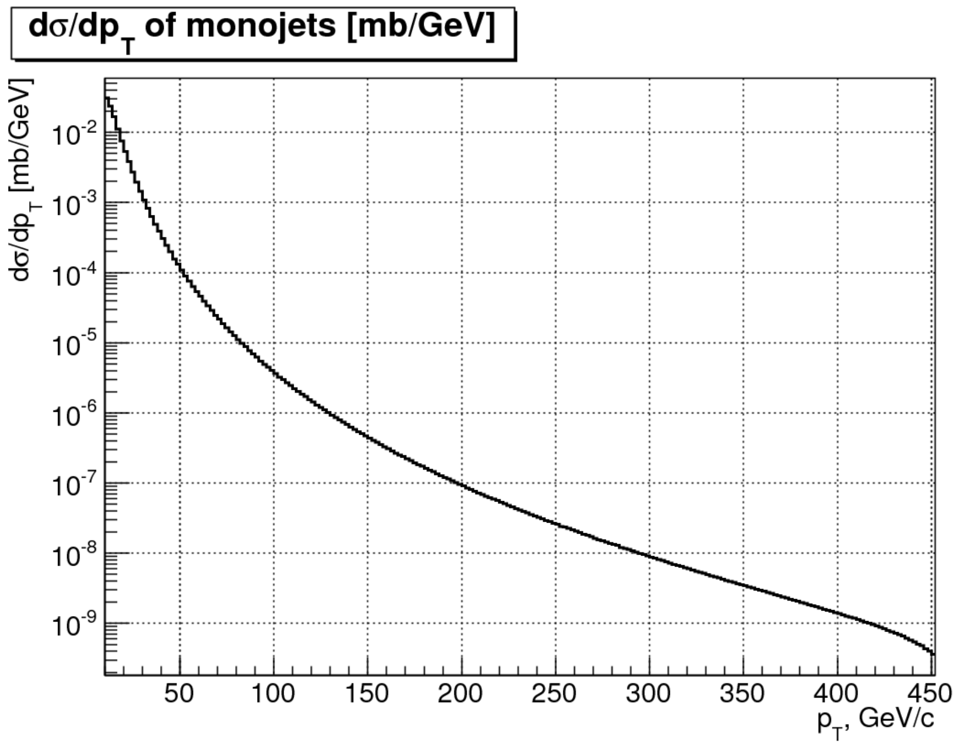

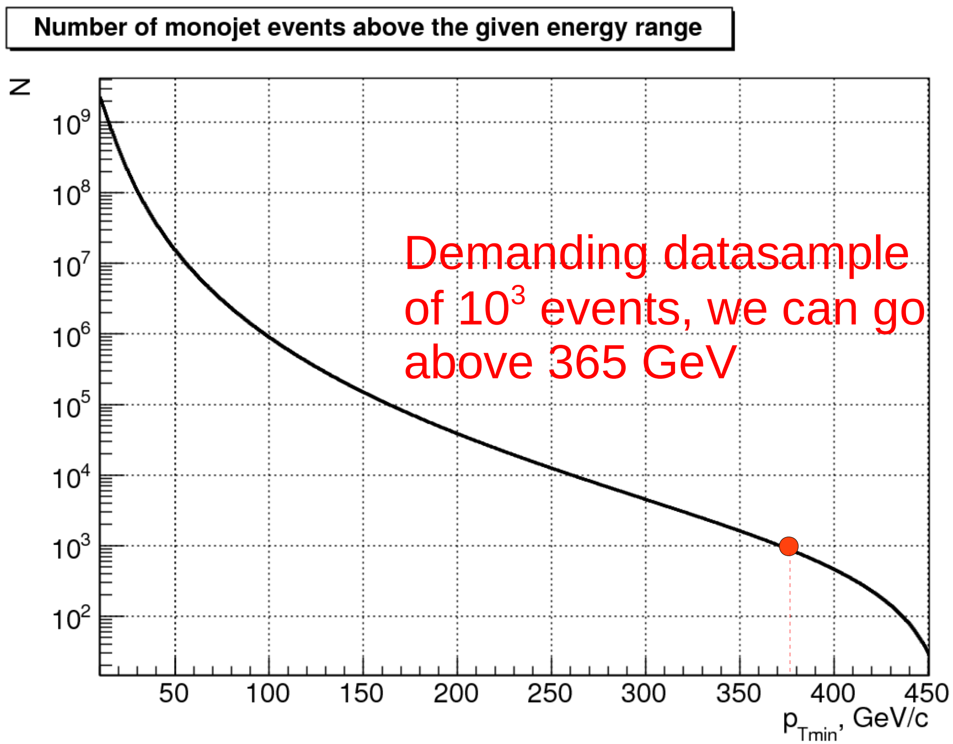

pp@7 TeV, L_{int}=0.1 pb^{-1}, acceptance: $\Delta\varphi=2\pi$, $|\eta|<0.9-R_{jet}$, $R_{jet}=0.4$

E_{min}, GeV	N_{events}
20	$2\ 10^8$
50	$2\ 10^7$
100	10^6

Jet energy bias and resolution

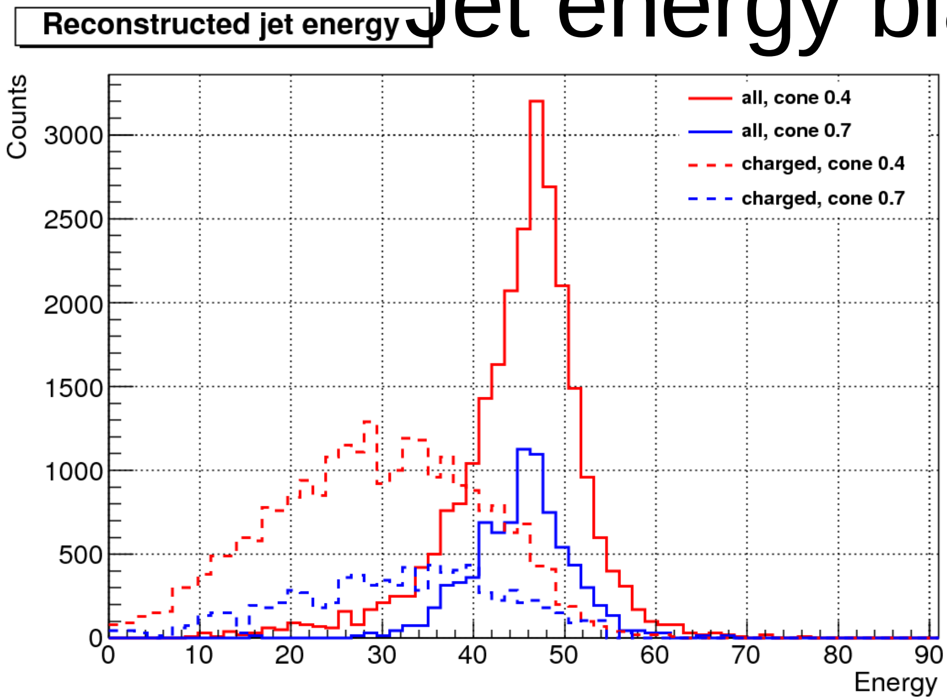

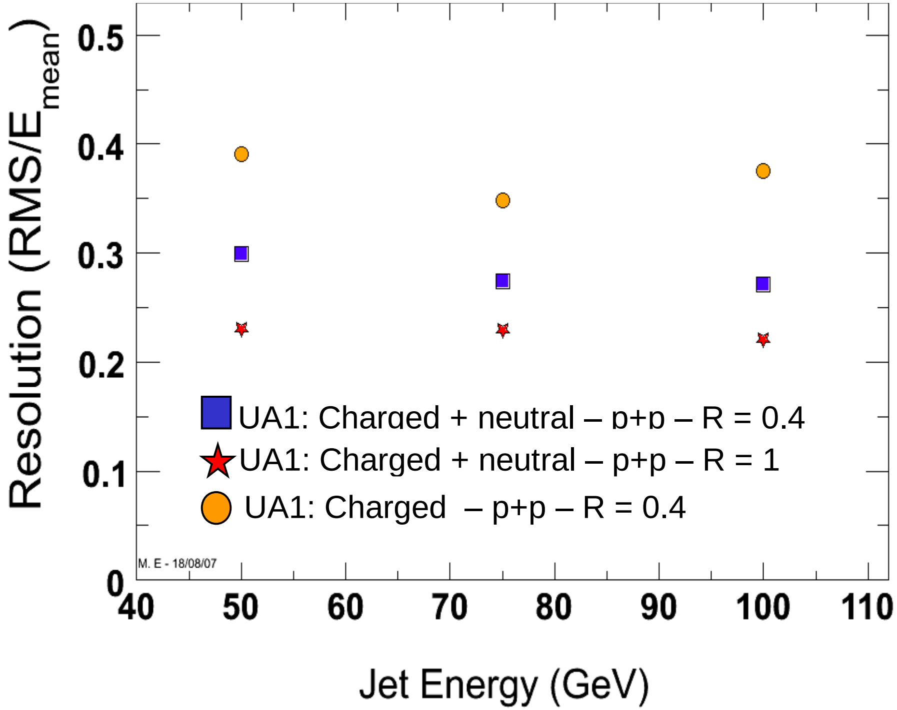

- Jets generated from 48 to 52 GeV and reconstructed with Pycell using different cone size
- Two effects: charge plus neutral fluctuations and out-of-cone fluctuations

- Full MC, jet finder UA1
- On top of charge plus neutral fluctuations and out-of-cone fluctuations we see the effect of the detector resolution

- Larger cone radius improves the jet energy resolution, but increases background
- Reconstruction of charged particles only biases the jet spectrum
- The expected resolution for jets with cone R=1 is around 20%, R=0.4 ≈ 30%, for R=0.4 charged only ≈ 40%

Dijet counting rates

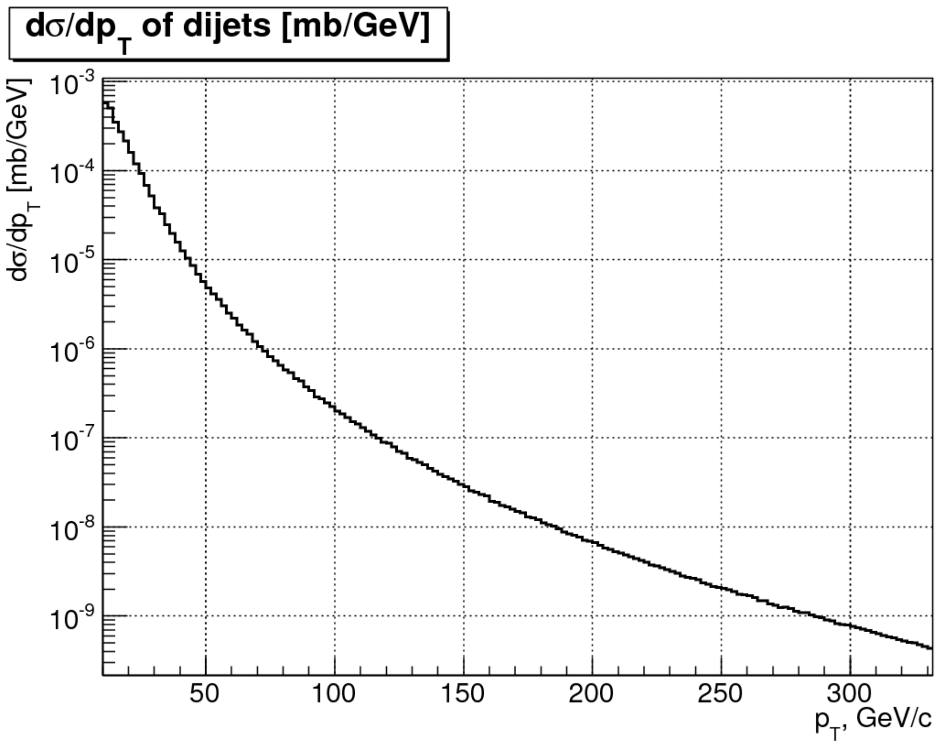

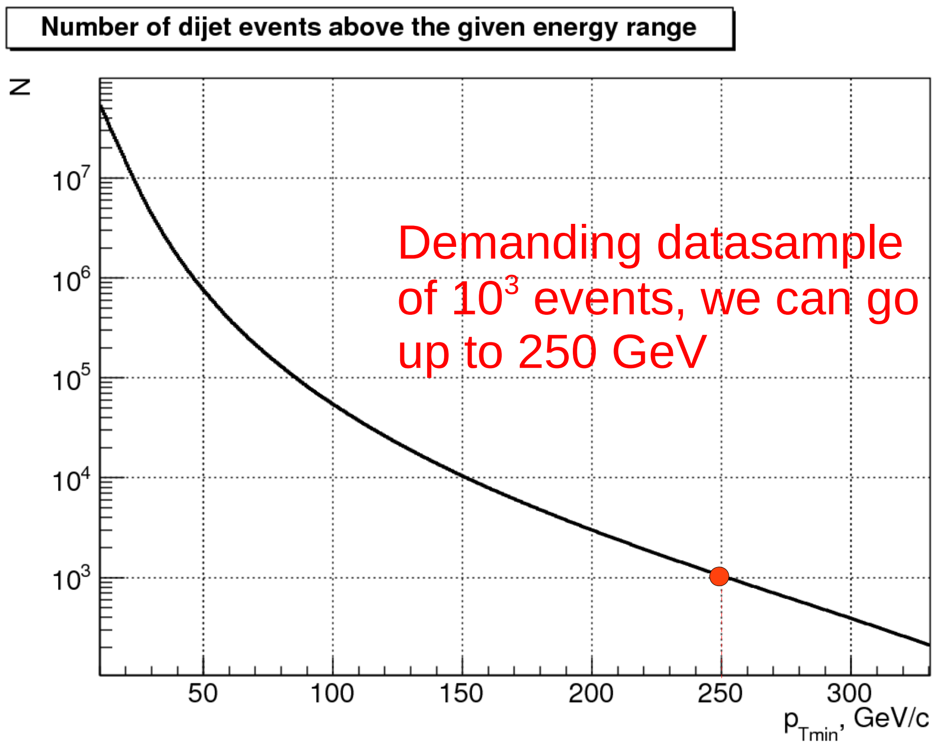

pp@7 TeV, L_{int}=0.1 pb^{-1}, acceptance: $\Delta\varphi=2\pi$, $|\eta|<0.9-R_{jet}$, $R_{jet}=0.4$

E_{min}, GeV	N_{events}
20	$7\ 10^6$
50	$8\ 10^5$
100	$5\ 10^4$

Comparison of dijet and monojet energy resolution

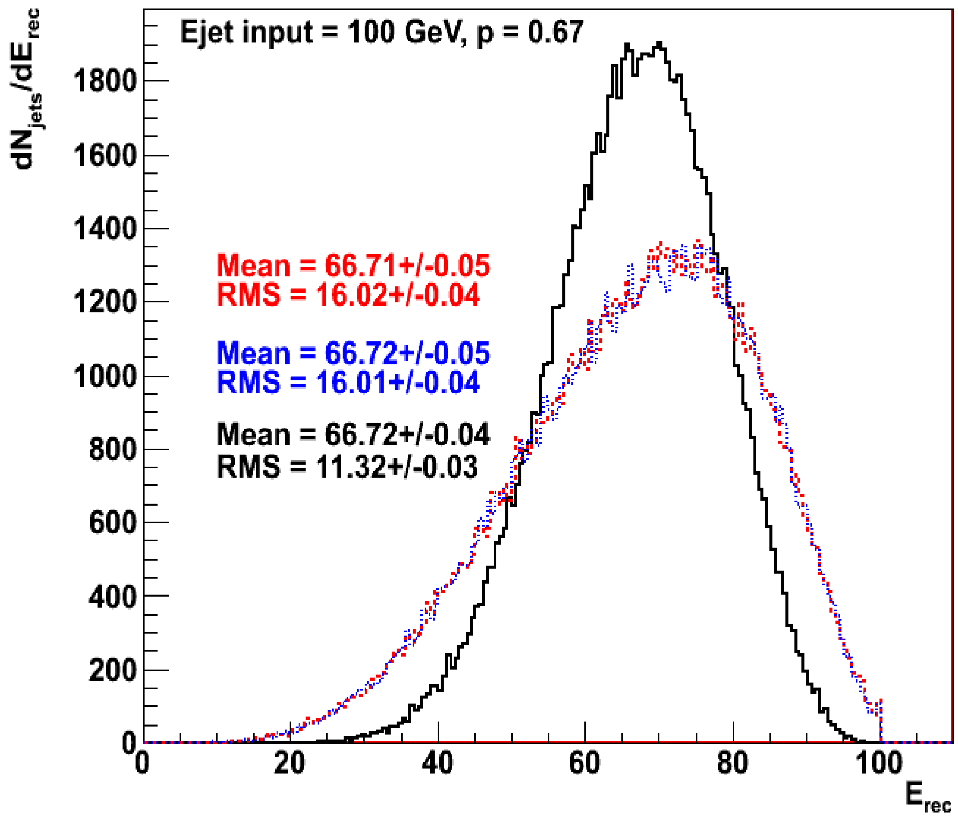

Samuel Lereah under the supervision of M. Estienne and T. Gousset

- •A simple probabilistic model with the probability to find charged particle – 2/3, neutral – 1/3
- •the particle energy distribution was taken exponential
- •In this model the expected resolution due to charge-to-neutral fluctuations is improved from 24 % with monojets to 17% for dijets (the improvement in √2 as expected)

Gamma-jets rates

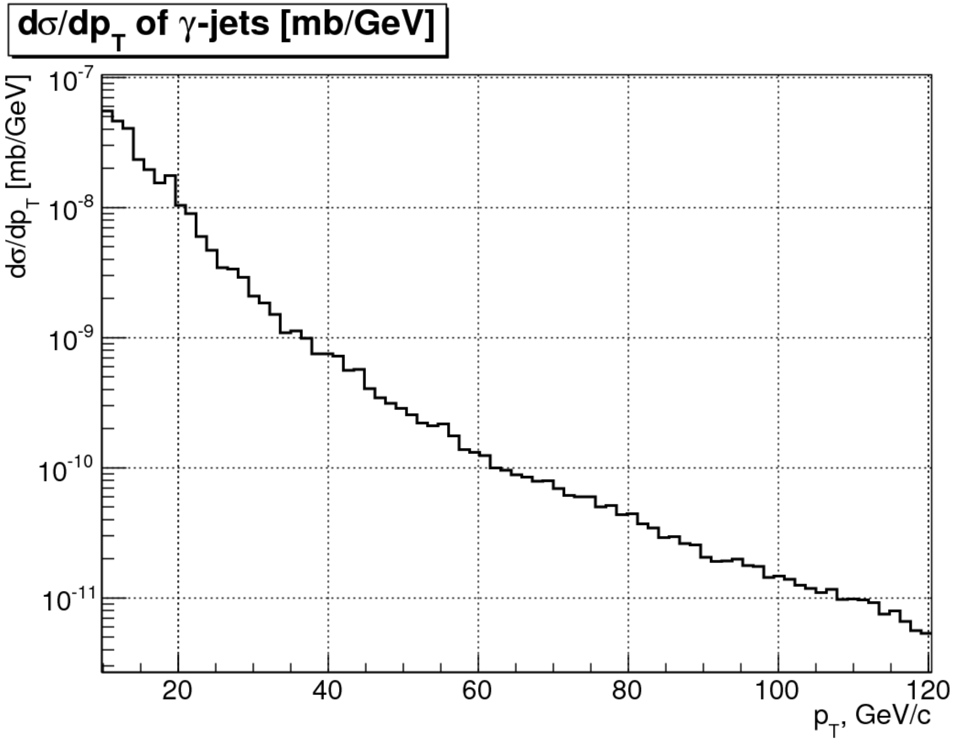

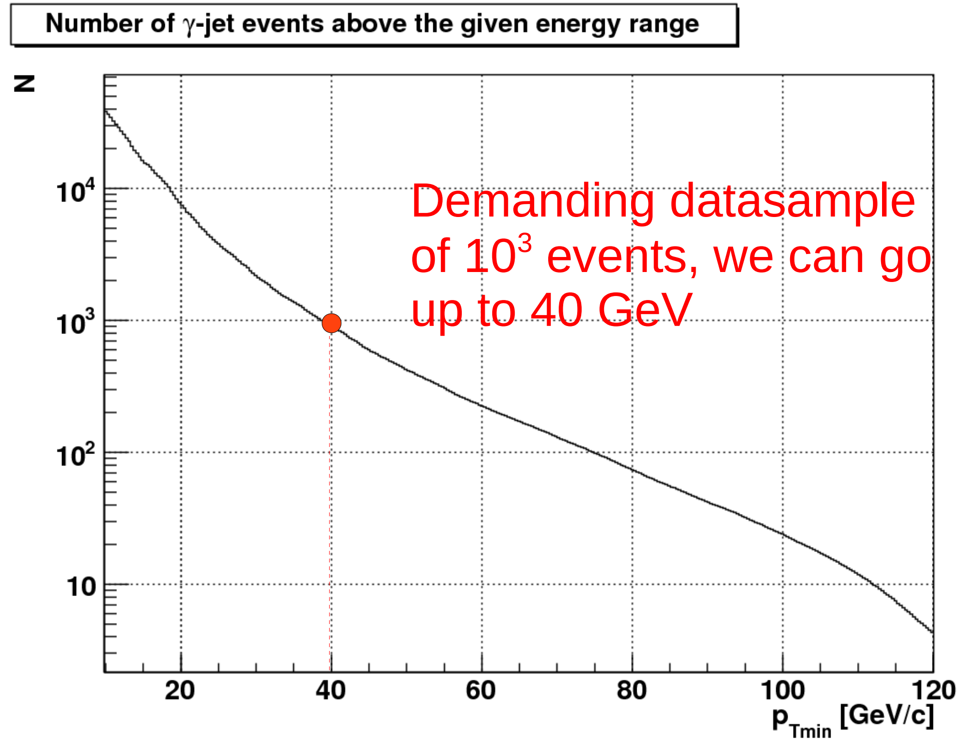

pp@7 TeV, L_{int}=1 pb^{-1}, γ acceptance (PHOS): 260<φ<320°, |η|<0.12

jet acceptance (EMCAL): 80<φ<120°, |η|<0.7-R_{jet}, R_{jet}=0.4

E_{min}, GeV	N_{events}
20	$8\ 10^3$
50	$5\ 10^2$
100	20

Photon PID for EMCAL

- Efficiency of photon identification is around 1 from 10 to 50 GeV
- Purity of the signal is more than 70% from 15 to 40 GeV
- The p_t region is compatible with the expected accessible region estimated in the γ-jet counting rates
- The results for efficiency and purity were obtained with shower shape analysis, we can extend the p_t range using isolation of the photon

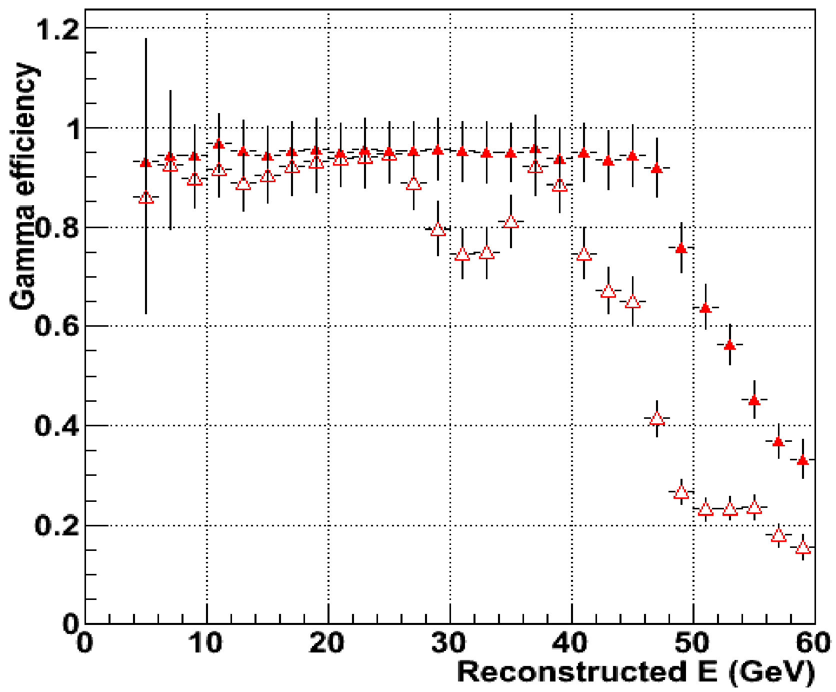

$$\text{Efficiency} = \frac{\text{N of } \gamma \text{ identified as } \gamma}{\text{N of real } \gamma}$$

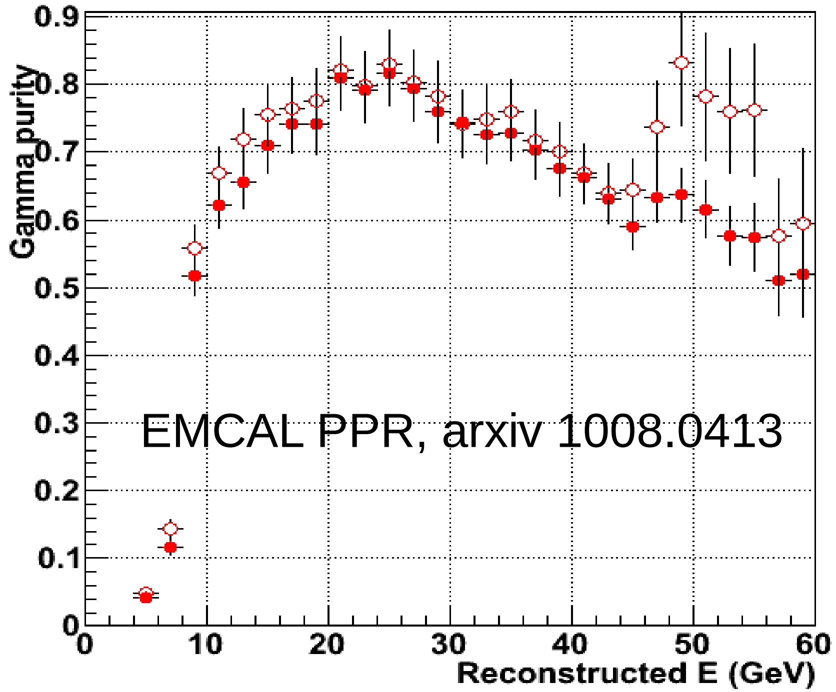

$$\text{Purity} = \frac{\text{N of } \gamma \text{ identified as } \gamma}{\text{N of particles identified as } \gamma}$$

ALICE and Intrajet radiation

ALICE can go to large ξ values

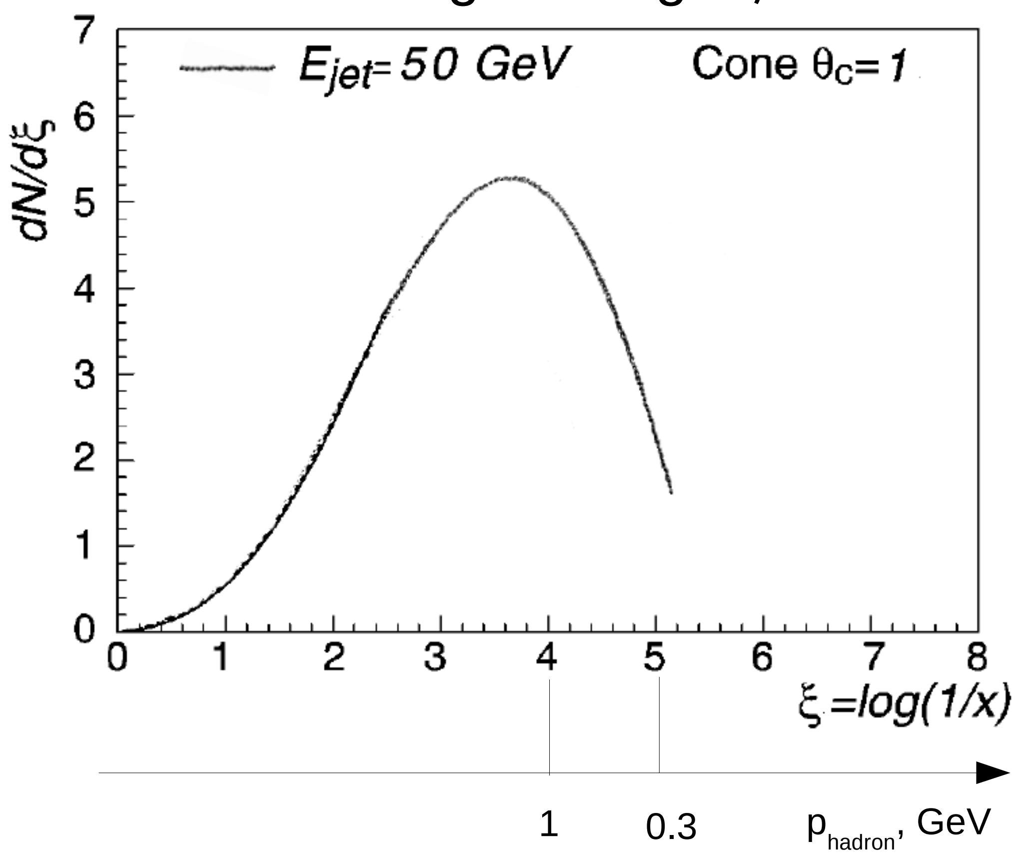

Combining information from different event topologies we can extend both upper and lower accessible p_t regions for jets.

Conclusion

- We aim for selecting the optimal event topology which is most sensitive for intrajet radiation.
- Speaking about event topology, one has to keep in mind that for having large statistics we pay with the energy resolution (mono- and dijets).
- On the contrary, having good energy resolution (tagging jet with gamma) has a drawback of decreasing statistics.
- In the MLLA, HBP and k_t distributions are derived perturbatively, the region where such derivations are justified is above 50 GeV.
- In ALICE we can go in the low hadron momentum region where non-perturbative effects dominate.
- ALICE capabilities to study intrajet radiation can be promising.

Perspectives

- Apply detector efficiency/resolution to fast MC and study their influence on jet finding efficiency, jet energy resolution within Pycell, sensitivity to fragmentation function (HBP).

- Analyze full MC with gamma-jet and jet-jet events, apply available photon and π_0 identification and jet finding algorithms. Optimize event selection and algorithms for HBP measurements.

- Study sensitivity of the ALICE detector for HBP measurements (ξ_0, peak width).

- Estimate expected statistical and systematic errors.

- Apply developed analysis to real pp@7 TeV data.


Thank you for attention!

Backup

ALICE particle identification capabilities

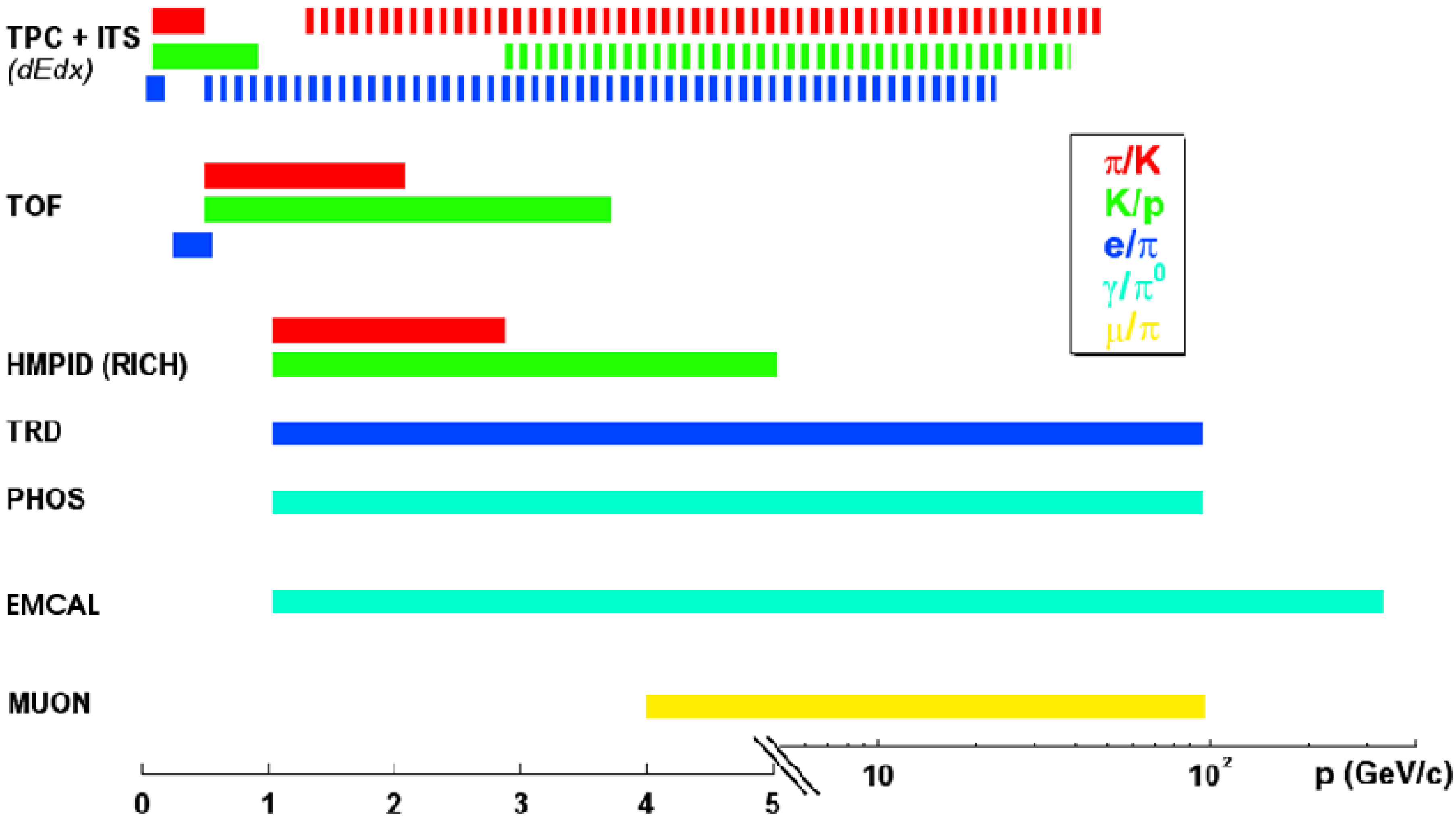

Identification of particles can be performed in a wide p_t range

Outlook of previous experiments

What was already measured?

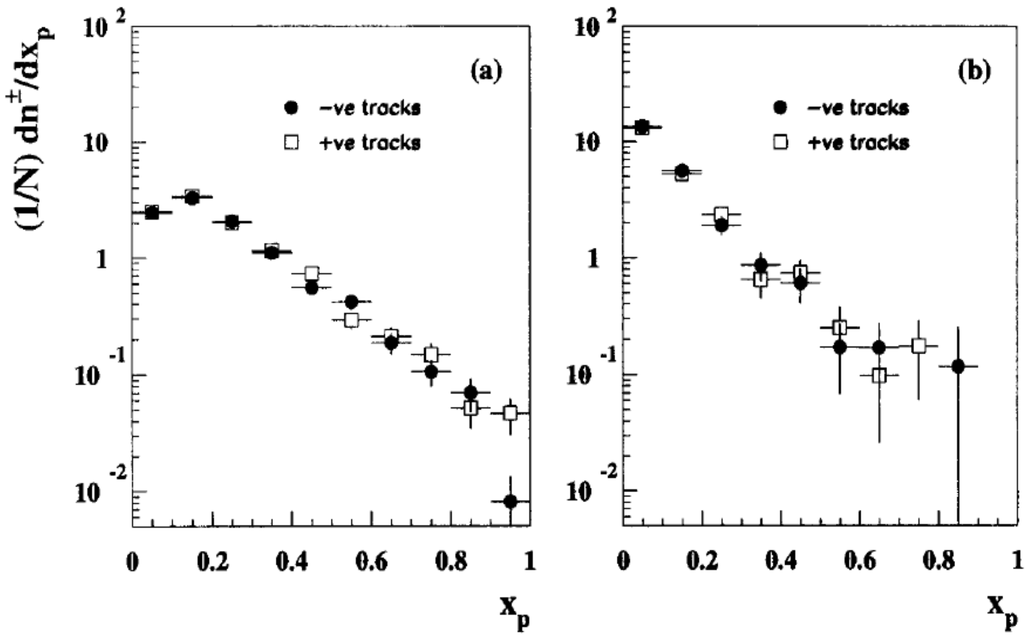

Fig. 3. The fragmentation functions, $D^{\pm}(x_p)$, for the current hemisphere of the Breit frame shown separately for positive and negative tracks, for (a) the low Q^2 and (b) the high Q^2 sample with statistical errors only.

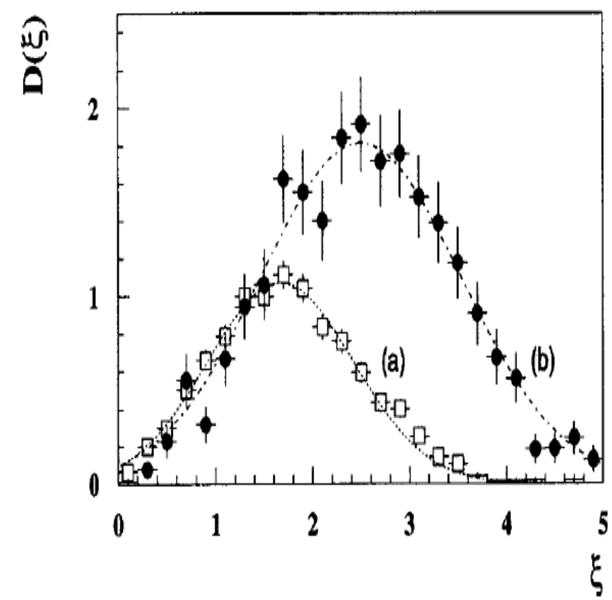

Fig. 4. The fragmentation functions for the current hemisphere of the Breit frame, $D(\xi)$, for (a) the low Q^2 and (b) the high Q^2 sample, with statistical errors only and with simple Gaussian fits superimposed.

Fragmentation function $D(x_p)$

H1 Collaboration. Nuclear Physics B 445 (1995) 3-21

H1: *D(ξ)* peak position and width

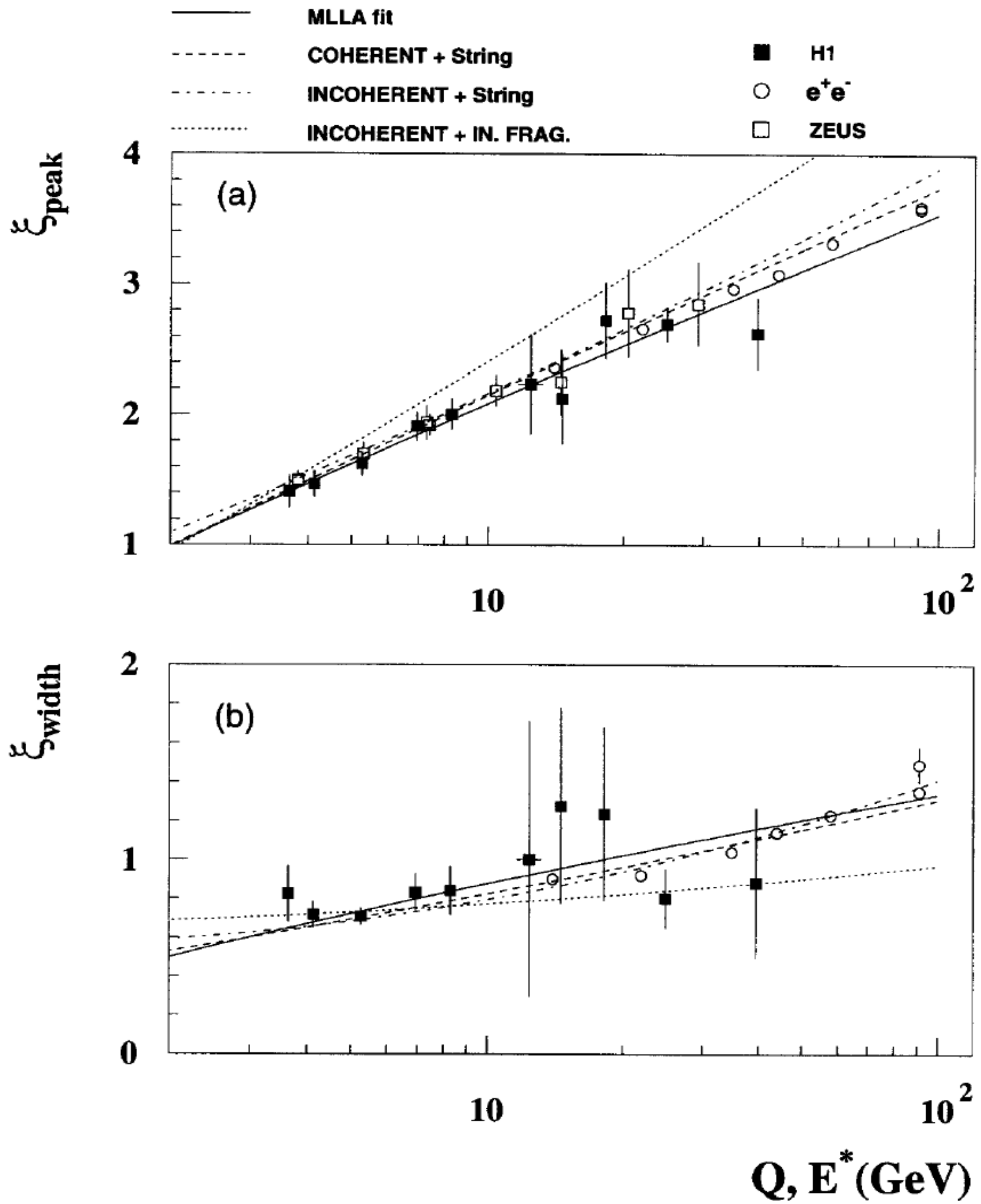

H1, ZEUS: average particle multiplicity in a jet

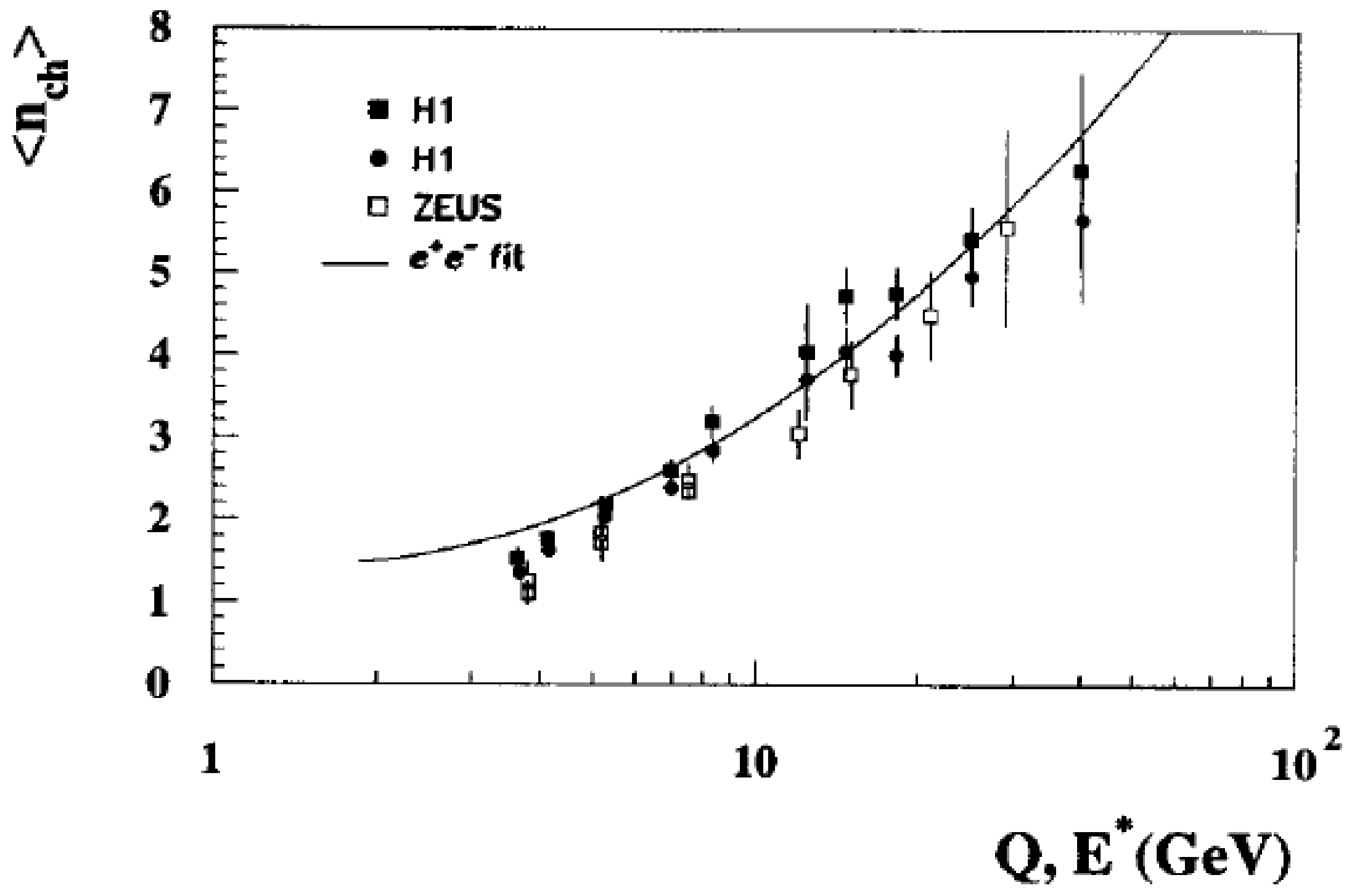

Average charged particle multiplicity in the current region of the Breit frame for data of H1, ZEUS and e^+e^-.

CDF, ZEUS, TASSO, L3, OPAL

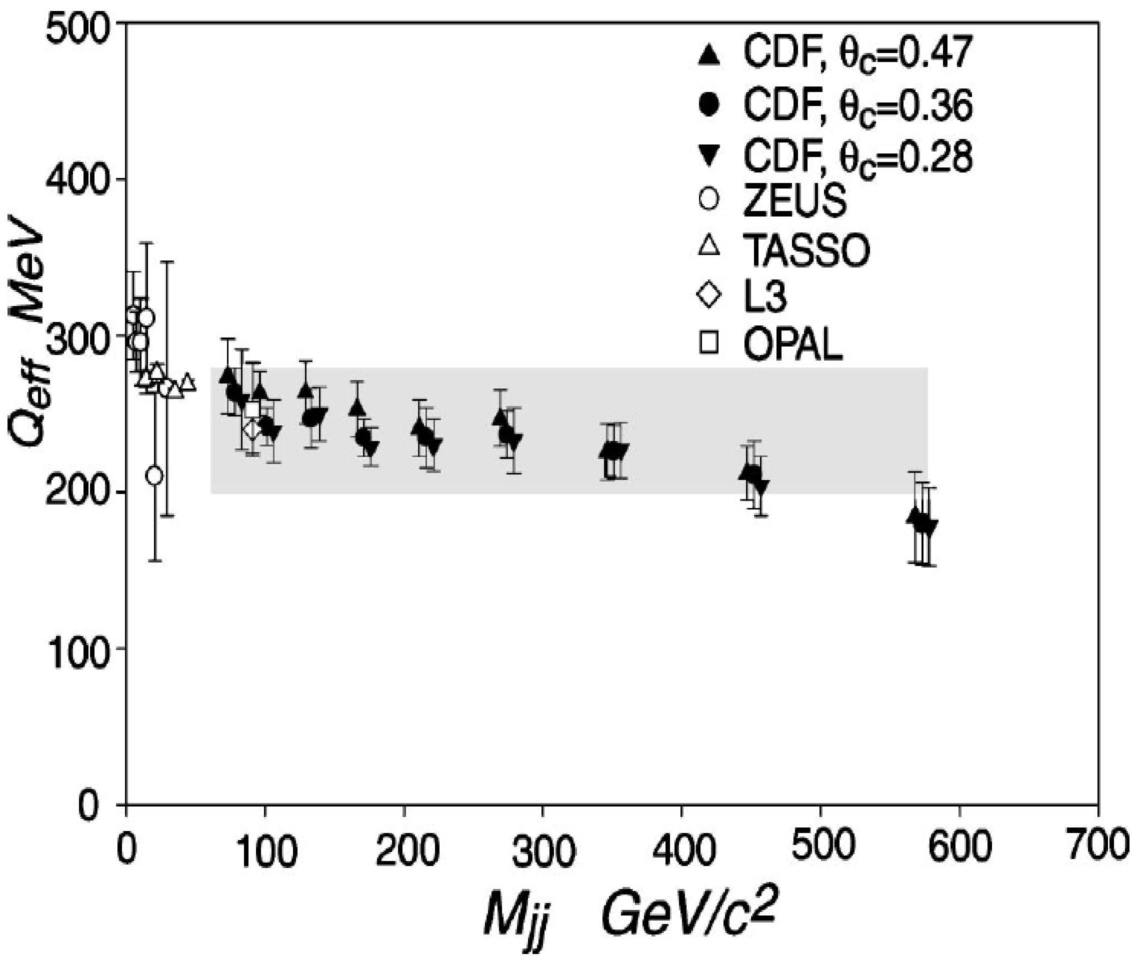

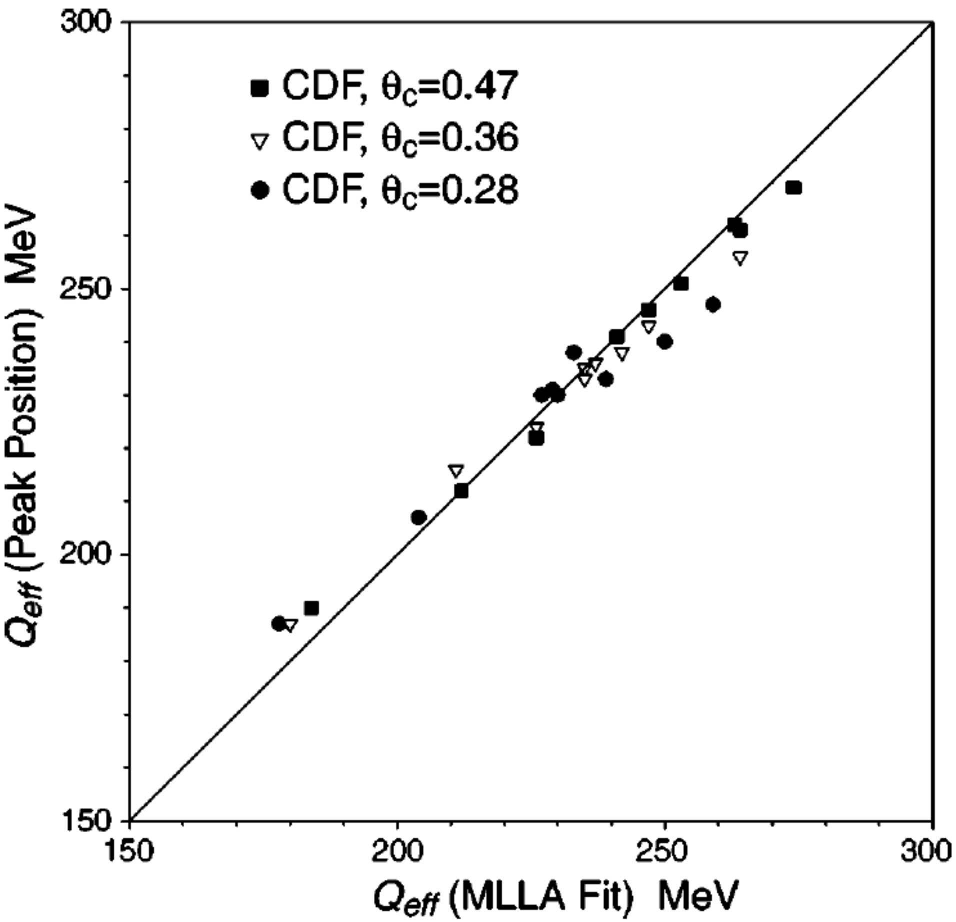

Q_{eff} measurement